Analysis of a Three-Dimensional Arbitrarily Shaped Dielectric or Biological Body Inside a Rectangular Waveguide

JOHNSON J. H. WANG, MEMBER, IEEE

Abstract—**This paper presents a method for the analysis of three-dimensional arbitrarily shaped dielectric obstacles inside a rectangular waveguide. The numerical computation involves a dyadic Green's function containing a double infinite series, which is evaluated by a partial summation technique.**

I. Introduction

WAVEGUIDE obstacles and discontinuities, including the dielectric type to be discussed in this paper, are long standing problems in electromagnetic theory. Many of them, essentially two dimensional, have been solved and were summarized by Marcuvitz [1]. The general three-dimensional discontinuity problems, however, remain unsolved in spite of the advent of modern high-speed digital computers and the method of moments [2] which permit treatment of problems not solvable by exact methods. Upon reviewing the status of numerical techniques for passive microwave devices, Silvester and Csendes [3] observed in 1974, "not a single truly three-dimensional solution has been published" for waveguide discontinuity problems. This statement is apparently still valid today.

This lack of published research activities in three-dimensional waveguide discontinuities has been in many circumstances due to the deficiencies of the Green's functions in the waveguide region. A dyadic Green's function for the rectangular waveguide was presented by Tai in 1972 [4] and later revised by the same author in 1973 [5]. Tai's expression includes a double infinite series summing over the contributions from all the individual waveguide modes. Recalling the simple expression of the free space Green's function, one immediately recognizes the greater complexity in the waveguide case.

This paper presents a successful use of the dyadic Green's function in the analysis of the electromagnetic problem of a three-dimensional arbitrarily shaped dielectric or biological body inside a rectangular waveguide. In the process, the extremely slow convergence of the double infinite series in the Green's function had to be modified by means of a partial summation technique. The immediate application of this new analytical technique is in microwave waveguide enzyme inactivation in neuro-chemical research [6]. Extension of this technique to highly conductive obstacles is feasible but may require modification of the volume integral into a surface expression.

Manuscript received November 7, 1977; revised February 7, 1978. This work was supported by the Army Medical R&D Command under Grant DAMD17-77-G-9422.

The author is with the Engineering Experiment Station, Georgia Institute of Technology, Atlanta, GA 30332.

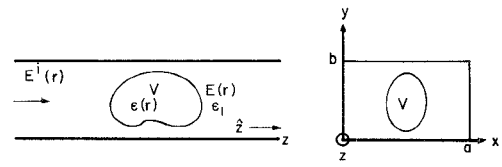

Fig. 1. A three-dimensional arbitrarily shaped heterogeneous dielectric body illuminated inside a rectangular waveguide.

II. The Integral Equation and the Dyadic Green's Function

The problem to be considered is shown in Fig. 1, in which a three-dimensional arbitrarily shaped heterogeneous dielectric or biological body is electromagnetically illuminated in a rectangular waveguide. The dielectric body has a permittivity distribution of $\epsilon(\boldsymbol{r})$, where $\boldsymbol{r}$ is a positional vector. Outside the volume V occupied by the dielectric body, the permittivity is homogeneous and is denoted by ϵ_1. Free space permeability μ_0 is assumed for both the dielectric body and the medium outside V.

The time function $e^{-j\omega t}$, where t and ω are time and radian frequency, is used in all the equations in this paper for ready comparison with Tai's work [4], [5]. Since the $e^{j\omega t}$ convention is perhaps more widely used, a comment on the conversion of the equations to this convention is justified at this point. For the $e^{j\omega t}$ convention, one merely changes to $-j$ all the j's appearing in the equations in this paper.

In Fig. 1, $\boldsymbol{E}(\boldsymbol{r})$ denotes the electric field intensity at $\boldsymbol{r}$ and $\boldsymbol{E}^i(\boldsymbol{r})$ denotes the field intensity at $\boldsymbol{r}$ with the dielectric body replaced by the medium ϵ_1. The scattered field is defined as

$$\boldsymbol{E}^s(\boldsymbol{r}) = \boldsymbol{E}(\boldsymbol{r}) - \boldsymbol{E}^i(\boldsymbol{r}). \tag{1}$$

The volume equivalence principle can be shown to be valid in the bounded as well as the unbounded space. As a result, the problem as depicted in Fig. 1 is equivalent everywhere to a homogeneous waveguide with ϵ_1, μ_0, and with volume current density

$$\boldsymbol{J}(\boldsymbol{r}) = -j\omega\left[\epsilon(\boldsymbol{r}) - \epsilon_1\right]\boldsymbol{E}(\boldsymbol{r}). \tag{2}$$

0018-9480/78/0700-0457$00.75

It follows from the theorem of superposition that the electric field radiated from $\boldsymbol{J}(\boldsymbol{r})$ is equal to $\boldsymbol{E}^s(\boldsymbol{r})$. Therefore,

$$\boldsymbol{E}^s(\boldsymbol{r}) = j\omega\mu_0 \int_V \bar{\boldsymbol{G}}_e(\boldsymbol{r},\boldsymbol{r}') \cdot \boldsymbol{J}(\boldsymbol{r}')\, dV' \tag{3}$$

where $\bar{\boldsymbol{G}}_e$ is the dyadic Green's function of the electric type and

$$\bar{\boldsymbol{G}}_e(\boldsymbol{r},\boldsymbol{r}') = \bar{\boldsymbol{G}}_{e0}(\boldsymbol{r},\boldsymbol{r}') - \frac{1}{k_1^2}\hat{z}\hat{z}\,\delta(\boldsymbol{r},\boldsymbol{r}') \tag{4}$$

where δ denotes a three-dimensional Dirac delta function, $\hat{z}$ denotes a unit vector along z, $k_1 = \omega\sqrt{\epsilon_1 \mu_0}$, and $\bar{\boldsymbol{G}}_{e0}$ is defined below. The term involving δ had not been included in Tai's earlier work [4] until 1973 [5] and has been a subject of recent discussions [5], [7], [8]. $\bar{\boldsymbol{G}}_{e0}$ was not explicitly expressed in the literature except by Rahmat-Samii [7]. However, Rahmat-Samii's expression has a number of errors in the print. For the clarity of the present discussion and the convenience of future references, it is desirable to present it in the following long form:

$$\begin{aligned}
\bar{\boldsymbol{G}}_{e0}(\boldsymbol{r},\boldsymbol{r}') = {} & \frac{j}{2abk_1^2} \sum_{m=0}^{\infty} \sum_{n=0}^{\infty} \frac{\epsilon_{0n}\epsilon_{0m}}{k_{mn}} e^{jk_{mn}|z-z'|} \\
& \cdot \left\{ \hat{x}\hat{x}\left[k_1^2 - \left(\frac{m\pi}{a}\right)^2 \right] \cos\frac{m\pi x}{a} \cos\frac{m\pi x'}{a} \right. \\
& \cdot \sin\frac{n\pi y}{b} \sin\frac{n\pi y'}{b} + \hat{y}\hat{y}\left[k_1^2 - \left(\frac{n\pi}{b}\right)^2 \right] \sin\frac{m\pi x}{a} \sin\frac{m\pi x'}{a} \\
& \cdot \cos\frac{n\pi y}{b} \cos\frac{n\pi y'}{b} + \hat{z}\hat{z}\left[\left(\frac{m\pi}{a}\right)^2 + \left(\frac{n\pi}{b}\right)^2 \right] \\
& \cdot \sin\frac{m\pi x}{a} \sin\frac{m\pi x'}{a} \\
& \cdot \sin\frac{n\pi y}{b} \sin\frac{n\pi y'}{b} + \hat{x}\hat{y}\left[-\left(\frac{m\pi}{a}\right)\cdot\left(\frac{n\pi}{b}\right) \right] \\
& \cdot \cos\frac{m\pi x}{a} \sin\frac{m\pi x'}{a} \\
& \cdot \sin\frac{n\pi y}{b} \cos\frac{n\pi y'}{b} + \hat{y}\hat{x}\left[-\left(\frac{m\pi}{a}\right)\cdot\left(\frac{n\pi}{b}\right) \right] \\
& \cdot \sin\frac{m\pi x}{a} \cos\frac{m\pi x'}{a} \\
& \cdot \cos\frac{n\pi y}{b} \sin\frac{n\pi y'}{b} + \hat{y}\hat{z}\left[\pm jk_{mn}\frac{n\pi}{b} \right] \sin\frac{m\pi x}{a} \sin\frac{m\pi x'}{a} \\
& \cdot \cos\frac{n\pi y}{b} \sin\frac{n\pi y'}{b} + \hat{z}\hat{y}\left[\mp jk_{mn}\frac{n\pi}{b} \right] \sin\frac{m\pi x}{a} \sin\frac{m\pi x'}{a} \\
& \cdot \sin\frac{n\pi y}{b} \cos\frac{n\pi y'}{b} + \hat{z}\hat{x}\left[\mp jk_{mn}\frac{m\pi}{a} \right] \sin\frac{m\pi x}{a} \cos\frac{m\pi x'}{a} \\
& \cdot \left. \sin\frac{n\pi y}{b} \sin\frac{n\pi y'}{b} + \hat{x}\hat{z}\left[\pm jk_{mn}\frac{m\pi}{a} \right] \cos\frac{m\pi x}{a} \sin\frac{m\pi x'}{a} \right\}, \qquad \text{for } z \gtrless z'
\end{aligned} \tag{5}$$

where

$$\epsilon_{0n} = \begin{cases} 1, & \text{if } n = 0 \\ 2, & \text{otherwise} \end{cases}$$

$$\boldsymbol{r} = \text{field point} = (x,y,z)$$

$$\boldsymbol{r}' = \text{source point} = (x',y',z')$$

$$k_{mn} = \begin{cases} |(k_1^2 - k_c^2)^{1/2}|, & \text{if } k_{mn} \text{ is real} \\ j|(k_c^2 - k_1^2)^{1/2}|, & \text{if } k_{mn} \text{ is imaginary} \end{cases}$$

where

$$k_c^2 = \left(\frac{m\pi}{a}\right)^2 + \left(\frac{n\pi}{b}\right)^2.$$

Equations (1)–(4) can be manipulated to yield the following integral equation:

$$j\omega\mu_0 \int_V \bar{\boldsymbol{G}}_{e0}(r,r') \cdot \boldsymbol{J}(\boldsymbol{r})\, dV' + \frac{\boldsymbol{J}(\boldsymbol{r})}{j\omega[\epsilon(\boldsymbol{r}) - \epsilon_1]} + \frac{J_z(\boldsymbol{r})\hat{z}}{j\omega\epsilon(\boldsymbol{r})} = -\boldsymbol{E}^i(\boldsymbol{r}) \tag{6}$$

where J_z is the z component of $\boldsymbol{J}$. The unknown $\boldsymbol{J}$ in (6) can then be solved by the method of moments [2] which transforms the integral equation into a set of linear equations readily solvable by means of a digital computer.

III. Solution by the Method of Moments

Although there exists a number of methods by which an integral equation can be solved numerically, the complexity of three-dimensional geometry can hardly tolerate further complication in the computational process. Even in the much simpler case of plane wave incidence and unbounded free space, only point matching together with rectangularly sided cells has been attempted for the volume type of integral equation [9]. Fortunately, this unsophisticated process has been found to be capable of producing good numerical results. Thus point matching with rectangularly sided cells is employed in the present analysis.

The volume V occupied by the dielectric body is first divided into L equal rectangular-sided cells ΔV_1–ΔV_L, each of which has constant dimensions Δx, Δy, and Δz. The electric field, assumed to be uniform inside the lth cell, is designated as $\boldsymbol{E}(\boldsymbol{r}_l)$, where $\boldsymbol{r}_l$ represents the center of the lth cell. The equivalent current in (2) can then be expressed as

$$\boldsymbol{J}(\boldsymbol{r}) = \sum_{l=1}^{L} \sum_{k=1}^{3} J_l^k \boldsymbol{B}_l^k(\boldsymbol{r}) \tag{7}$$

where $\boldsymbol{B}_l^k$ is a basis function defined as

$$\boldsymbol{B}_l^k(\boldsymbol{r}) = \hat{u}_k P^l(\boldsymbol{r}), \qquad k = 1,2,3 \text{ or } x,y,z \tag{8}$$

$\hat{u}_k$ in (8) denotes a unit vector, and

$$P^l(\boldsymbol{r}) = \begin{cases} 1, & \text{for } \boldsymbol{r} \text{ in } \Delta V_l \\ 0, & \text{elsewhere.} \end{cases} \tag{9}$$

The weighting function is defined as

$$W_q^p(\boldsymbol{r}) = \delta(\boldsymbol{r}-\boldsymbol{r}_q)\hat{u}_p, \qquad p=1,2,3. \tag{10}$$

The scalar product between $\boldsymbol{f}$ and $\boldsymbol{g}$ is defined as

$$(\boldsymbol{f},\boldsymbol{g}) = \int_V \boldsymbol{f}\cdot\boldsymbol{g}\, dv. \tag{11}$$

We can generate a set of linear equations by first substituting (7) into (6) and then performing a scalar product on the resulting equation with the weighting function of (10) for $p=1,2,3$ and $q=1,\cdots,L$. This moment generating procedure leads to the following set of equations:

$$\sum_{k=1}^{3}\sum_{l=1}^{L} J_l^k A_{kl}^{pq} = C^{pq}, \qquad p=1,2,3;\ q=1,\cdots,L \tag{12}$$

where

$$C^{pq} = -\boldsymbol{E}^i(\boldsymbol{r}_q) \tag{13}$$

$$A_{kl}^{pq} = j\omega\mu_0 Q_{lq}^{pk} + \frac{\delta_q^l}{j\omega}\left[\frac{\delta_k^p}{\epsilon(\boldsymbol{r}_q)-\epsilon_1} + \frac{\delta_3^k\cdot\delta_3^p}{\epsilon(\boldsymbol{r}_q)}\right]. \tag{14}$$

δ_k^p in (14) is the Kronecker delta, being 1 when $p=q$ and 0 otherwise, and

$$Q_{lq}^{pk} = \int_{\Delta V_l} G_{e0}^{pk}(\boldsymbol{r}_q,\boldsymbol{r}')\, dV' \tag{15}$$

where G_{e0}^{pk} is the (p,k) component of the dyad $\bar{\boldsymbol{G}}_{e0}$. The integration in (15) can be carried out to yield

$$Q_{lq}^{pk} = \frac{j}{2abk^2}\sum_{n=0}^{\infty}\sum_{m=0}^{\infty}\frac{\epsilon_{0n}\epsilon_{0m}}{k_{mn}} IQF_{mn}^{pk} \tag{16}$$

where

$$F_{mn}^{pk} = \left[\text{the } (m,n)\text{th term of } G_{e0}^{pk}\right]\cdot e^{-jk_{mn}|z_q-z_l|} \tag{17}$$

$$Q = \frac{4ab}{n\pi m\pi}\sin\frac{n\pi\Delta X_l}{2a}\sin\frac{m\pi\Delta Y_l}{2b} \tag{18}$$

and I in (16) depends on the index pk. For pk being (1,3), (2,3), (3,1), (3,2), where (1,2,3) corresponds to (x,y,z), we have

$$I = \begin{cases} \pm\dfrac{2}{k_{mn}} e^{jk_{mn}|z_q-z_l|}\sin\left(k_{mn}\dfrac{\Delta z_l}{2}\right), & \text{if } z_q \gtrless z_l + \dfrac{\Delta z_l}{2} \\ \dfrac{2}{k_{mn}} e^{jk_{mn}\Delta z_l/2}\sin\left[k_{mn}(z_q-z_l)\right], & \text{otherwise.} \end{cases} \tag{19}$$

For other pk indices, we have

$$I = \begin{cases} \dfrac{2}{jk_{mn}}\left\{\cos\left[k_{mn}(z_q-z)\right]e^{jk_{mn}\Delta z_l/2}-1\right\}, & \\ \qquad\qquad \text{if } z_l+\dfrac{\Delta z_l}{2} \geqslant z_q \geqslant z_l-\dfrac{\Delta z_l}{2} & \\ \dfrac{2}{k_{mn}}\sin\left(k_{mn}\dfrac{\Delta z_l}{2}\right)e^{jk_{mn}|z_q-z_l|}, & \text{otherwise.} \end{cases} \tag{20}$$

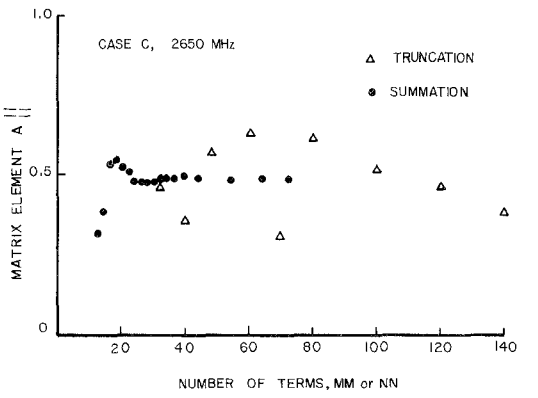

Fig. 2. Comparison of convergence between direct truncation and partial summation.

As can be seen in (14)–(20), the matrix element A_{kl}^{pq} involves a double infinite series which does not converge rapidly unless $|z_q-z_l|$ is large. When $p=q$ as is the case for the self cells which are the diagonal matrix elements $|z_q-z_l|=0$ and the series convergence is extremely slow. As an example, Fig. 2 shows that no sign of convergence is exhibited even after 140×140 terms are used in the summation. Thus the computation of the matrices can not be carried out by a simple truncation of the series.

This computational difficulty can be surmounted by direct summation of the part of the infinite series which contains terms nonvanishing with increasing M and N. This partial summation transforms a matrix element of a double infinite series into a single infinite series or even into an expression of closed form, which can be truncated for computation. Fig. 2 shows that convergence is achieved with about 20×20 terms for the partial-summation technique, which is significant improvement over the direct truncation method. For most off-diagonal matrix elements, direct truncation is satisfactory because of the predominant influence of the exponential terms with the argument of $jk_{mn}|z_q-z_l|$ or $jk_{mn}\Delta z_l/2$ as shown in (19) and (20). As a result of these exponential terms which rapidly decrease with m and n, off-diagonal matrices with nonvanishing $|z_l-z_q|$ can be computed with a finite series truncated according to a precision criterion established by the value of $jk_{mn}|z_q-z_l|$. Depending on the value of $|z_q-z_l|$, approximately 16×8 up to 21×12 terms were used for m and n in the examples reported in this paper.

The partial summation technique is tedious but straightforward. The portion of the infinite series which consists of terms slowly convergent with m and n are summed by means of the following formulas [10]:

$$\sum_{k=1}^{\infty}\frac{\sin kx}{k} = \frac{\pi-x}{2}, \qquad [0<x<2\pi]$$

$$\sum_{k=1}^{\infty}\frac{k\sin ka}{k^2+a^2} = \frac{\pi}{2}\frac{\sin ha(\pi-x)}{\sin ha\pi}, \qquad a^2>0,\ 0<x<2\pi$$

$$\sum_{k=0}^{\infty}\frac{k\sin kx}{k^2-a^2} = \pi\frac{\sin\left\{a\left[(2m+1)\pi-x\right]\right\}}{2\sin a\pi},$$

$$2m\pi \leqslant x \leqslant (2m+2)\pi, \qquad a \text{ being noninteger}$$

$$\sum_{k=1}^{\infty} \frac{\cos kx}{k^2+a^2} = \frac{\pi}{2a} \frac{\cos h(\pi - x)}{\sin ha\pi} - \frac{1}{2a^2}, \qquad 0 < x \leqslant 2\pi$$

$$\sum_{k=1}^{\infty} \frac{\cos kx}{k^2-a^2} = \frac{1}{2a^2} - \frac{\pi}{2} \frac{\cos a[(2m+1)\pi - x]}{a \sin a\pi},$$

$$2m\pi \leqslant x \leqslant (2m+2)\pi, \qquad a \text{ being noninteger.}$$

The explicit expressions for the matrix elements after partial summation are too complex to be presented in this paper and the interested readers are referred to [11] for further details. Their computation on a digital computer is efficient since only logical expressions and elementary algebraic and transcendental functions are involved.

IV. Numerical Examples and Supporting Measurements

A method for analyzing the electromagnetic problem of a three-dimensional arbitrarily shaped body inside a rectangular waveguide has been presented. A Fortran IV computer program was written for the numerical testing of this approach. Measurements were also conducted to compare with the theoretical prediction. Several cases were studied and satisfactory results have been obtained. Validation of the theory and the computer program was achieved with numerical convergence tests as well as direct comparison with measured data, which included transmission-reflection characteristics and thermographic heating patterns.

Three cases, as shown in Fig. 3, are presented in this paper. All of the test cases consist of homogeneous dielectric bodies with rectangular side walls aligned with the waveguide walls. This choice of geometry conformal to the Cartesian coordinates is mainly for the sake of simplicity in data management and should not result in any significant loss of generality as was noted in the free space case [9]. For highly conductive obstacles, the surface curvature of the obstacle plays a more important role and therefore should be treated with greater discretion.

It was noted that the linear cell dimensions should be $\lambda/2$ (λ being the free space wavelength divided by the square root of the dielectric constant) or less in order to yield accurate data. This observation had been reported in the free space case studied by Livesay and Chen [9] and later by Hagmann *et al.* [12]. Fig. 4 shows good agreement in the reflection and transmission properties of Case B between a 12-cell calculation and the measured data using a model made of silica compound. A 12-cell calculation from Case A, being also a case of low dielectric constant, yields a power reflection coefficient of 0.114 at 2.65 GHz, dropping down to 0.035 at 3.5 GHz, which was verified experimentally with a paraffin wax model.

While 12 cells are sufficient for the calculation of Cases A and B, many more cells are needed for Case C, which has a high dielectric constant. Case C was originally intended to be a phantom model for simulating muscle tissue. The model was made by mixing water, powdered polyethylene, and "super stuff," a modeling compound manufactured by Wham-O Co., San Gabriel, CA. The dielectric constant and loss tangent were then measured at various frequencies. There were difficulties in achieving and maintaining the desired dielectric properties of the phantom model and, as a result, only the repeatable measured data are shown in Fig. 5, in which comparisons are also made for three calculations using different numbers of subvolume cells. The measured data in Fig. 5

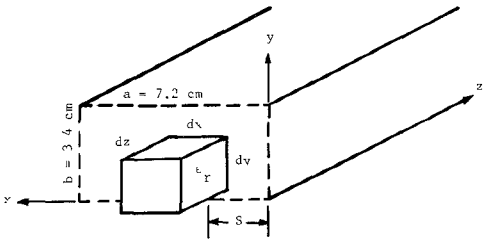

CASE	ε_r	d_x	d_y	d_z	S
A	2.25 + j0.00045	4.9	1.4	3.05	1.15
B	4.25 + j0.0425	4.0	1.25	2.0	1.0
C	49.5 + j16.8	3.2	2.65	2.0	2.93

ε_r = relative dielectric constant at 2.65 GHz
d_x, d_y, d_z, S in cm.

Fig. 3. Configurations of the three cases studied.

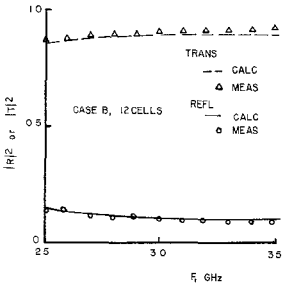

Fig. 4. Comparison between calculated and measured reflection and transmission characteristics for Case B of Fig. 3 which is of low dielectric constant.

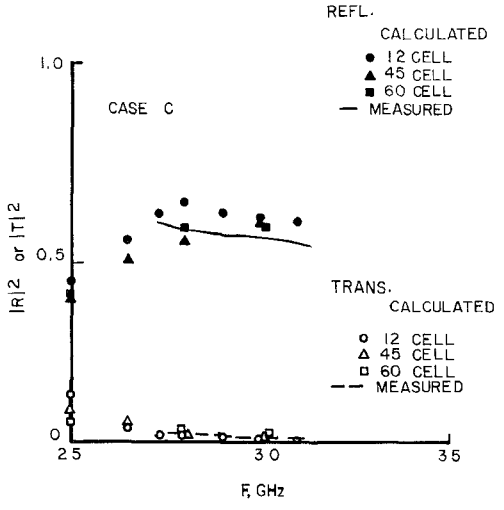

Fig. 5. Comparison between measurements and calculations of various numbers of cells for Case C of a high dielectric constant.

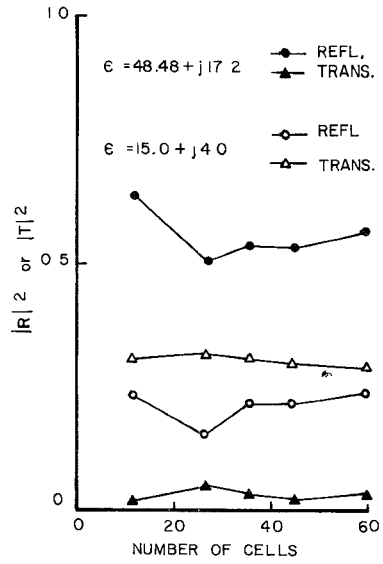

Fig. 6. Convergence of transmission and reflection properties for Case C with high and medium dielectric constants at 2.8 GHz.

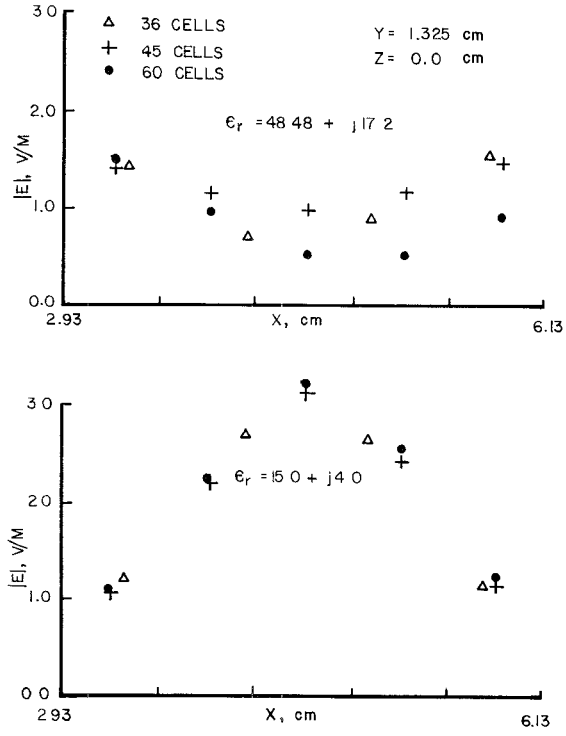

Fig. 7. Convergence of field distribution for Case C at 2.8 GHz with high and medium dielectric constants.

agree reasonably with the calculation. The 12-cell configuration is obviously overly crude, yet the results are in gross agreement with those of finer configurations. Note that in the 45-cell calculation the y dimension of each cell is 0.8833 cm, which is about 0.52λ at 2.5 GHz and 0.68λ at 3.1 GHz. Convergence becomes more rapid when the linear dimensions of the subvolume cells decrease to $\lambda/2$ or less.

The rapidity of convergence of the present model approach is further illustrated in Figs. 6 and 7. Fig. 6 shows the calculated power reflection and transmission coefficients versus the number of cells used for the geometry of Case C with two values of complex dielectric constant. In Fig. 7, the field distribution inside the dielectric body is compared for various numbers of subvolume cells used in the calculation. It has been noted that the convergence of field intensity is related to the profile of the field. When the field varies slowly with the coordinates, convergence is rapid. Fig. 7 presents typical situations with moderately varying fields. The favorable influence of the lower dielectric constant on the convergence of the field distribution is clearly demonstrated.

Dielectric bodies of high dielectric constant require not only a larger number of cells but also a greater number of terms in the Green's function series. This is due to the fact that the distance between adjacent cells is small because of the smaller size of the cells. The attenuation of higher order modes, being independent of the dielectric constant, decreases when the distances between adjacent cells centers are shortened. As a result, the calculation cost for cases of high dielectric constants increases rapidly with an increase in dielectric constant.

V. Concluding Remarks

A general three-dimensional waveguide dielectric obstacle has been successfully treated by employing the moment method on an integral equation involving a dyadic Green's function. This general method can be applied to a number of waveguide problems. An immediate extension of this technique would be to ferromagnetic obstacles. For highly conductive obstacles a surface-type Green's function may be more desirable.

Acknowledgment

The author wishes to express his gratitude to Dr. C. E. Ryan, Jr. and F. L. Cain, both at the Engineering Experiment Station of the Georgia Institute of Technology, and Dr. L. Larsen and Dr. R. H. Lennox, of Walter Reed Army Institute of Research, for their interest and support of this research.

References

[1] N. Marcuvitz, *Waveguide Handbook*. New York: McGraw-Hill, 1951.
[2] R. F. Harrington, *Field Computation by Moment Method*. New York: MacMillan, 1968.
[3] P. Silvester and Z. J. Csendes, "Numerical modeling of passive microwave devices," *IEEE Trans. Microwave Theory Tech.*, vol., MTT-22, pp. 190–201, Mar. 1974.
[4] C. T. Tai, *Dyadic Green's Functions in Electromagnetic Theory*, Scranton, PA: Intext Educational Publishers, 1972.
[5] C. T. Tai, "On the eigen-function expansion of dyadic Green's functions," *Proc. IEEE*, vol. 61, p. 480, Apr. 1973.
[6] R. H. Lenox, O. P. Gandhi, J. L. Meyerhoff, and H. M. Gove, "A microwave application for in vivo rapid inactivation of enzymes in the central nervous system," *IEEE Trans. Microwave Theory Tech.*, vol. MTT-24, pp. 58–61, Jan. 1976.
[7] Y. Rahmat-Samii, "On the question of computation of the dyadic Green's function at the source region in waveguides and cavities," *IEEE Trans. Microwave Theory Tech.*, vol. MTT-23, pp. 762–765, Sept. 1975.
[8] R. E. Collin, "On the incompleteness of E and H modes in wave guides," *Can. J. Phys.*, vol. 51, pp. 1135–1140, 1973.
[9] D. E. Livesay and K. M. Chen, "Electromagnetic fields induced inside arbitrarily shaped biological bodies," *IEEE Trans. Microwave Theory Tech.*, vol. MTT-22, pp. 1273–1280, Dec. 1974.

[10] I. S. Gradshteyn and I. W. Ryzhik, *Table of Integrals, Series and Products*. New York: Academic Press, 1965, pp. 38–40.
[11] J. J. H. Wang, "An analytical approach for use with waveguide enzyme-inactivation investigations," Final report, U. S. army Medical R & D Command Grant DAMD17-77-G-7422, Engineering Experiment Station, Georgia Institute of Technology, Jan. 1978.
[12] M. J. Hagmann, O. P. Gandhi, and C. H. Durney, "Upper bound on cell size for moment-method solutions," *IEEE Trans. Microwave Theory Tech.*, vol. MTT-25, pp. 831–832, Oct. 1977.

Method of Analysis and Filtering Properties of Microwave Planar Networks

GUGLIELMO D'INZEO, FRANCO GIANNINI, CESARE M. SODI, AND ROBERTO SORRENTINO, MEMBER, IEEE

Abstract—**A method of analysis of planar microwave structures, based on a field expansion in term of resonant modes, is presented. A first advantage of the method consists in the possibility of taking into account fringe effects by introducing, for each resonant mode, an equivalent model of the structure. Moreover, the electromagnetic interpretation of the filtering properties of two-port networks, particularly of the transmission zeros, whose nature has been the subject of several discussions, is easily obtained. The existence of two types of transmission zeros, modal and interaction zeros is pointed out. The first ones are due to the structure's resonances, while the second ones are due to the interaction between resonant modes. Several experiments performed on circular and rectangular microstrips in the frequency range 2–18 GHz have shown a good agreement with the theory.**

I. Introduction

AFTER THE STUDY of the transmission properties of microstrip lines, the great diffusion of microwave integrated circuits has led to the analysis of general planar circuits. To this purpose, analytical methods, applied to structures of simple geometry [1]–[3], and numerical methods, apt to the study of more complex geometries [4]–[6], have been developed. In both cases a magnetic wall model has been adopted for the structure because of the formidable boundary value problems. In such a way, however, one not only neglects the dispersion properties of the circuit, which are due to fringe effects, but often obtains erroneous results [7].

To overcome this difficulty, in the case of step discontinuities, i.e., of structures with separable geometry in rectangular coordinates, Menzel and Wolff [8] have recently proposed a method of analysis based on the correction of the magnetic wall model by means of frequency dependent effective parameters. However, it must be observed that effective parameters depend not only on the frequency, but also on the field distribution inside the structure. It is sufficient to instance the disk resonators for which Wolff and Knoppik [9] have shown a frequency dependent equivalent model to exist for each resonant mode, in such a way that a unique equivalent model for the structure cannot be defined. This fact strongly limits the applicability of all the analyses of microstrip structures presented until now. Considerable attention has been devoted to nonuniform lines, i.e., lines with continuously or not continuously varying cross sections. The existence of transmission zeros has been stressed both theoretically and experimentally. In the particular case of a double step discontinuity, the physical nature of such zeros has been discussed for a long time [2], [10]–[13] and they have been ascribed to the excitation of higher order modes of propagation in the line section between the two discontinuities. As will be shown below, such an interpretation, in our opinion, is not correct, also because transmission zeros are present in generic nonuniform lines where the EM field cannot propagate as exp $(-j\beta z)$.

In this paper an analysis of planar circuits based on the theory of resonant cavities is presented. Three important advantages are so obtained. The first consists in the possibility of introducing frequency dependent effective parameters for each resonant mode of the structure in such a way as to obtain an accurate characterization of its frequency behavior. The second is an electromagnetic interpretation of the network's filtering properties, particularly of the transmission zeros, is easily obtained and the above mentioned problems are clarified. Finally, the present method leads to the evaluation of the impedance matrix of the network in the form of a partial fraction expansion with the advantages pointed out by Silvester [6].

The analysis is limited to the important case of two-port networks, since the extension to the general case is

Manuscript received May 16, 1977; revised December 7, 1977. This work has been supported in part by the Consiglio Nazionale delle Ricerche (C. N. R.), Italy.

The authors are with the Istituto di Elettronica, Università di Roma, Rome, Italy.

0018-9480/78/0700-0462$00.75